AUTOMATIC CYCLE IDENTIFICATION IN TIDAL BREATHING SIGNALS

A Thesis by

Zuojun Wang

Bachelor of Science, Beijing University of Chemical Technology, 2008

Submitted to the Department of Electrical Engineering and Computer Science
and the faculty of the Graduate School of
Wichita State University
in partial fulfillment of
the requirement for the degree of
Master of Science

December 2010

AUTOMATIC CYCLE IDENTIFICATION IN TIDAL BREATHING SIGNALS

The following faculty members have examined the final copy of this thesis for form and content, and recommend that it be accepted in partial fulfillment of the requirement for the degree of Master of Science with a major in Electrical Engineering.

Yanwu Ding, Committee Chair

Douglas F. Parham, Committee Member

Hyuck M. Kwon, Committee Member

DEDICATION

To my parents, Bangyuan Xiang and Yaping Wang and Family

ACKNOWLEGEMENTS

I would like to thank my adviser, Dr. Yanwu Ding, for her support and guidance. I would like to give thanks to Dr. Douglas F. Parham provided us guidance and data for our research, and my thesis used this research data. I wish to express my appreciation to Dr. Hyuck M. Kwon. He gave me good suggestions when I had problems, and I also learned a lot from his classes and seminars.

I would like to thank my dear friends Kanghee Lee, Yu Bi and all the group members for their encouragement and support.

Outside of the lab, I have cherished the company of several friends throughout the past two years. In particular, I would like to thank Richard and Edithe Daeschner for their help, care and faith in me.

ABSTRACT

In this paper, we introduce a novel cycle identification algorithm using Matlab programming to automatically identify cycles in tidal breathing signals. The algorithm is designed in four steps using filtering, derivation, and other signal processing techniques. To verify the effectiveness of the proposed algorithm, its results are compared with those of cycles identified manually by a human coder. Simulations results show that despite the complexity of the respiratory signals, the proposed algorithm can identify cycles more correctly and more efficiently than cycles identified by hand-coding. This algorithm can serve as an important first step toward timely identification and coding of more complex respiratory signals, such as those underlying speech productions.

TABLE OF CONTENTS

LIST OF FIGURES

Figure

LIST OF ABBREVIATIONS/NOMENCLATURE

ACIA	Automatic Cycle Identification Algorithm
HCM	Hand-Coded Method

CHAPTER 1

INTRODUCTION

1.1 Motivation

The analysis of periodic and quasiperiodic waveforms typically involves some form of automatic cycle detection [1, 2, 3, 4, 5]. There are powerful algorithms available to isolate specific frequencies of interest in a given waveform; many of these provide readily available measurements [6, 7, 8]. In the case of physiological behavior, rate measurements are often used as summary statistics of the waveforms representing that behavior (e.g., number of breaths per minute) [9]. Unfortunately, cycle averaging techniques are often inadequate when it comes to describing complex behavior, particularly when that behavior changes over time [10, 11]. In the case of respiratory behavior, at least two factors preclude the use of simple cycle averaging: (a) the detection of individual and physiologically informative variation in chest wall kinematics, and (b) the discrimination of interpretable and uninterpretable cycles. Both of these factors are mitigated by the expertise of an experienced coder who can evaluate each cycle of a given waveform to determine which ones are acceptable, and then measure them accordingly. The downside to human visual coding and measurement is the time required to complete it. The twofold purpose of this inquiry is to describe an algorithm that automatically detects tidal breath cycles across a variety of human subjects and to compare the algorithm's performance to that achieved by an experienced human coder.

1.2 Contribution

In this paper, an automatic cycle identification algorithm is proposed to be used with tidal breath signals. The algorithm uses filtering and other signal processing techniques via the Matlab programming [12, 13]. To facilitate further analysis for tidal breath signals, the algorithm

produces the exact start time-instant for each cycle and isolates the distorted cycles due to artifacts. Simulations results have shown that, despite the inter- and intra-participant variability of the tidal breath signals, the proposed algorithm can identify tidal breath cycles correctly and efficiently. It can also isolate those portions of the signals negatively impacted by motion artifact.

1.3 Thesis Outline

The paper is organized as follows. Chapter 2 details the respiratory signals used for this analysis. Chapter 3 describes the proposed algorithm related to automatic cycle identification in the tidal breath signals. Chapter 4 shows the simulation results to compare the proposed Automatic Cycle Identification Algorithm (ACIA) with hand-coded results by the third author (Hand-Coded Method (HCM)). Chapter 5 concludes the paper.

CHAPTER 2

DATA COLLECTION SCHEMES AND TIDAL BREATH SIGNALS

2.1 Data Collection

The data used for analysis are a subset of respiratory kinematic data collected for a study exploring chest wall movement during conversational interaction. The participants were twenty healthy women who were American English speakers between 22 years, 8 months and 34 years, 8 months old (the mean is 25 years and 4 months) and randomly assigned to dyads. The participants in each dyad took turns in the role of speaker and listener across a total of sixteen segments, resulting in a total of 160 segments across the ten dyads (one segment was lost during the data recording phase). Each participant's respiratory movements were measured using a respiratory inductive plethysmograph (Inductotrace®, Ambulatory Monitoring, Inc., Ardsley, NY). The signal of interest for this inquiry was the tidal breath signal produced by each participant in the role of listener.

The Inductotrace® system produced two signals representing rib cage and abdomen excursions, which were digitized at a maximum rate of 2 kHz. The sum of these two excursion signals was calibrated to a known volume and adjusted using least-squares estimation. The sum waveform was digitally downsampled to a rate of 100 Hz with a low-pass filter cutoff of 5 Hz (Butterworth). The mean duration of the signal was 114.78 seconds (standard deviation = 15.70 seconds).

2.2 Examples of Tidal Breath Signals

Figure 1 shows two 12-second segments of tidal breath signals. Each tidal breath cycle is composed of an inspiratory phase and an expiratory phase, with the two phases being delineated by the maximum peak of each cycle. Whereas tidal breath cycles are similar in their overall

shape and quasi-periodic nature, the segments demonstrate some degree of inter- and intra-participant variability. The inspiratory start and the expiratory end of each cycle are indicated by the vertical dashed lines. The start and end points are identified by viewing each respiratory sum waveform within a signal analysis program, zooming in on each cycle, and labelling the points that correspond to physiological respiratory phases. Hand-coding the signal by an experienced coder is time-consuming and may be less precise than an algorithm-based identification system, depending on the resolution at which the signal is viewed and coded.

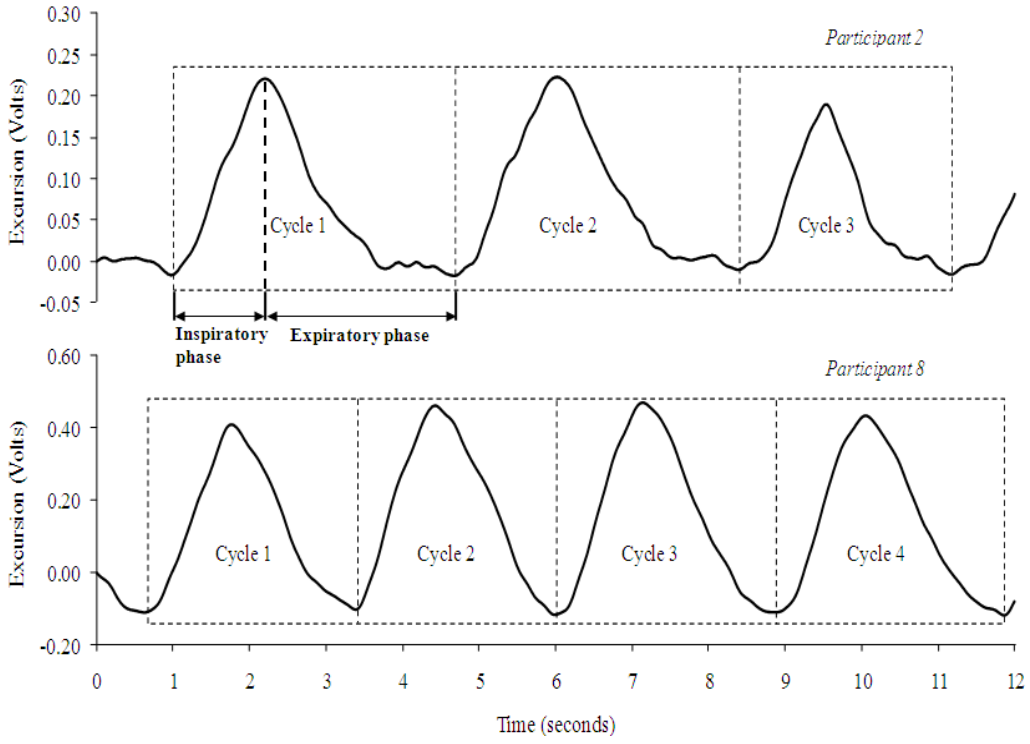

Figure 1. Examples of tidal breath signals

Another example of the variability of tidal breath cycles is provided in Figure 2. What is apparent is the difference in the ending segments of the expiratory phases among participants (indicated by the dotted boxes). The ripples within the signals are normal variations in chest wall movement, and a particular pattern can often be characteristic of an individual's tidal breath

signal. It is important than any algorithm-based coding system be able to adjust to and manage this variability across individual signals.

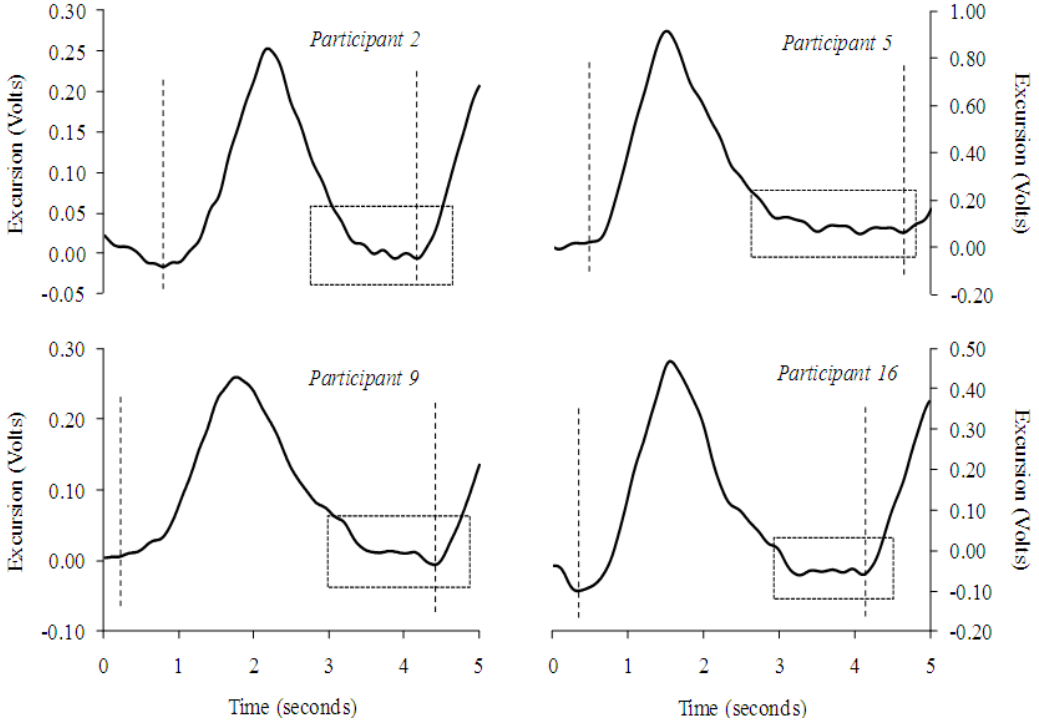

Figure 2. Examples of individual tidal breath cycles

As with most physiological signals, the signal representing chest wall movement is prone to distortion by motion artifact, which is caused primarily by gross-motor movement and/or shifts in posture that are transferred to the sensors. Figure 3 shows two examples of how motion artifact can negatively impact the interpretability of the tidal breath signal. The unwanted displacement or distortion of the signal makes it impossible to determine the end point of the previous cycle, which is equivalent to the starting point of the subsequent cycle. The motion artifact can also introduce short-term upward or downward trends in the signal (as can be seen in the lower graph of Figure 3). It is not difficult for a coder to identify, isolate, and remove from analysis the presence of motion artifact in the tidal breath signal; an algorithm-based coding system must be able to do the same.

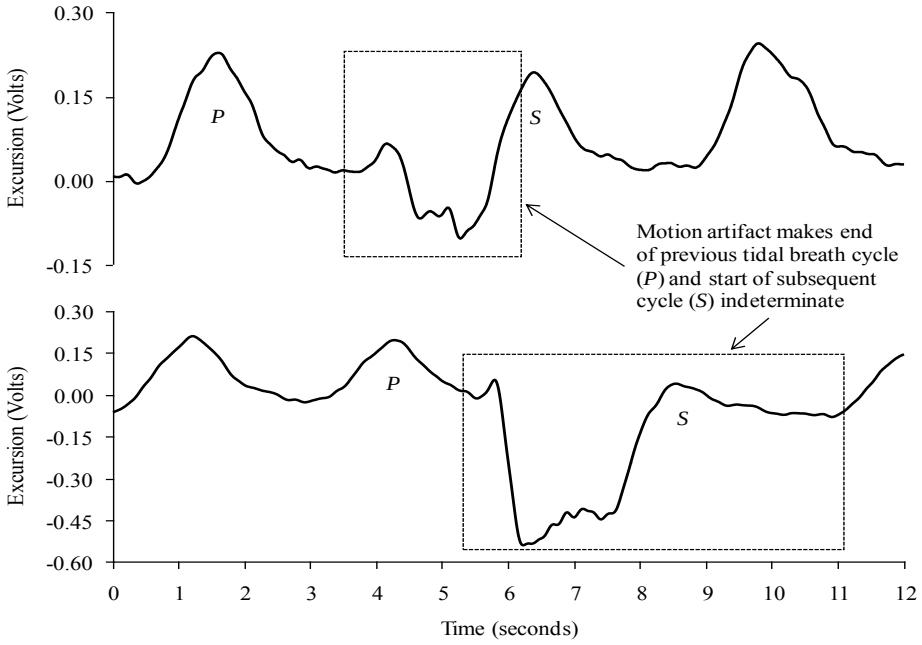

Figure 3. Examples of the impact of motion artifact on tidal breath signals

CHAPTER 3

AUTOMATIC CYCLE IDENTIFICATION ALGORITHM

The proposed automatic cycle identification algorithm includes four steps as shown in Figure 4. The first three steps focus on cycle identifications including determining the total number of cycles and their exact start times. The fourth step detects and isolates the distorted cycles that cannot be used for the purpose of respiratory signal analysis. To make the proposed algorithm universal to all the respiratory data collected, detailed criteria have been used in step II and III. An overview for the four steps is given with illustrating figures, followed by a detailed description for each step in the algorithm.

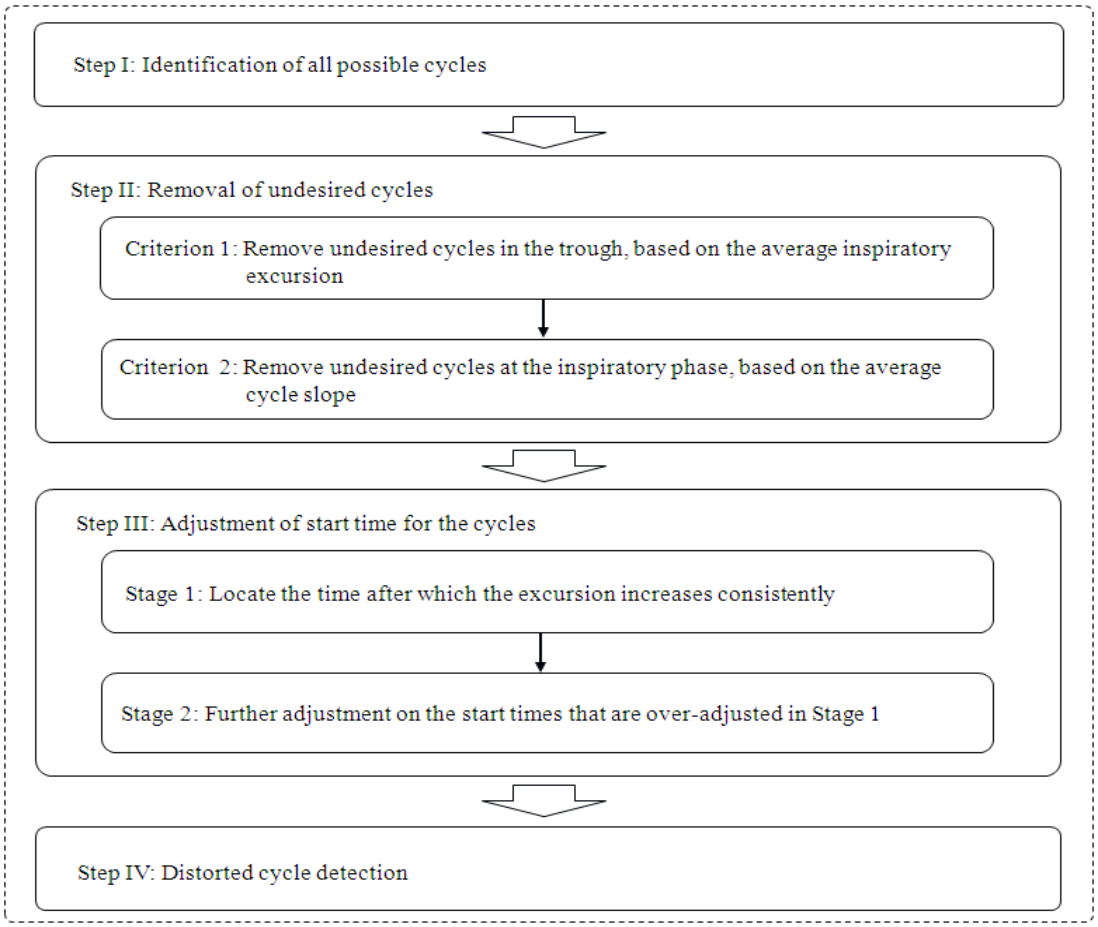

Figure 4. Diagram of the automatic cycle identification algorithm

There are some important notations using in this algorithm: The uppercase letter represents the total number of data samples in a tidal breath data file. The excursion voltage value at the -th sample is denoted by , where is the sampling period in seconds (the sampling period in the analyzed data was seconds). The total number of cycles is denoted by , where subscript "A" is used to indicate the step and stage addressed in the proposed cycle identification algorithm. Typical values for "A" are I, II, or III. The start time for the -th tidal breath cycle is denoted by . The cycles are indexed consecutively; therefore, the start time for the -th cycle is also the ending-time for the -th cycle. Notation represents the maximum excursion voltage value in the -th cycle. and denote, respectively, the minimum values in the inspiratory and expiratory phases in the -th cycle (and are usually not identical), subscripts L and R are used because the inspiratory phase is in the left portion of a cycle and the expiratory phase is in the right portion. and are also referred to as the left and right minimum in the -th cycle.

3.1 Overview of the Algorithm

1) Step I: Identification for All Possible Cycles: The goal of Step I is to identify all possible cycles in the tidal breath signals by looking for possible start time-instants via initial processing techniques, including decimation, derivation, and interpolation. The cycles are marked by vertical lines drawn at the start time for each cycle, as indicated in the first plot in Figure 5. As the cycles are numbered consecutively from the beginning of the data, the start time of a cycle is also the end time of the previous cycle. It is clear from Figure 5 that the initial processing techniques in Step I also identifies a number of cycles between two normal or desired cycles. As these cycles do not represent any normal tidal breath cycles, we refer them as "undesired cycles" and remove them. This task is carried out in Step II.

2) Step II: Removal of Undesired Cycles: It is observed that the undesired cycles identified in Step I can be generally classified into two patterns based on their locations, as shown in the second plot in Figure 5. The patterns are represented by the dashed and dotted-dashed cycle identification lines, respectively. Two criteria are proposed to remove the undesired cycles in each pattern using various characteristics of the data such as the local maxima, minima, and slope. After the undesired cycles are removed, the cycles are renumbered; therefore, the index of the last cycle is also the total number of desired cycles in the data file.

3) Step III: Adjustment on Start Time for the Cycles: By implementing Step II, all the desired cycles are identified successfully by their start times and marked by vertical lines. However, there is often a small offset between the correct start time and that marked by the vertical line obtained in Step II. Therefore, Step III is designed to find the exact start time of each cycle and adjust the corresponding identification line. A two-stage adjustment procedure is used by identifying the time at which the next inspiratory phase starts and examining the local minimum in the neighborhood of the trough between two adjacent cycles. The third plot in Figure 5 shows the results obtained in Step III.

4) Step IV: Distorted Cycle Detection: As mentioned in Section II, some cycles in the signals are distorted as those indicated by dashed lines in the last plot in Figure 5. The distorted cycles have an undesired upwards or downwards displacement. Those cycles cannot be used for purpose of future analysis because it is impossible to tell the ending point of the previous cycles. Step 4 is designed to detect, isolate and remove them from the data file.

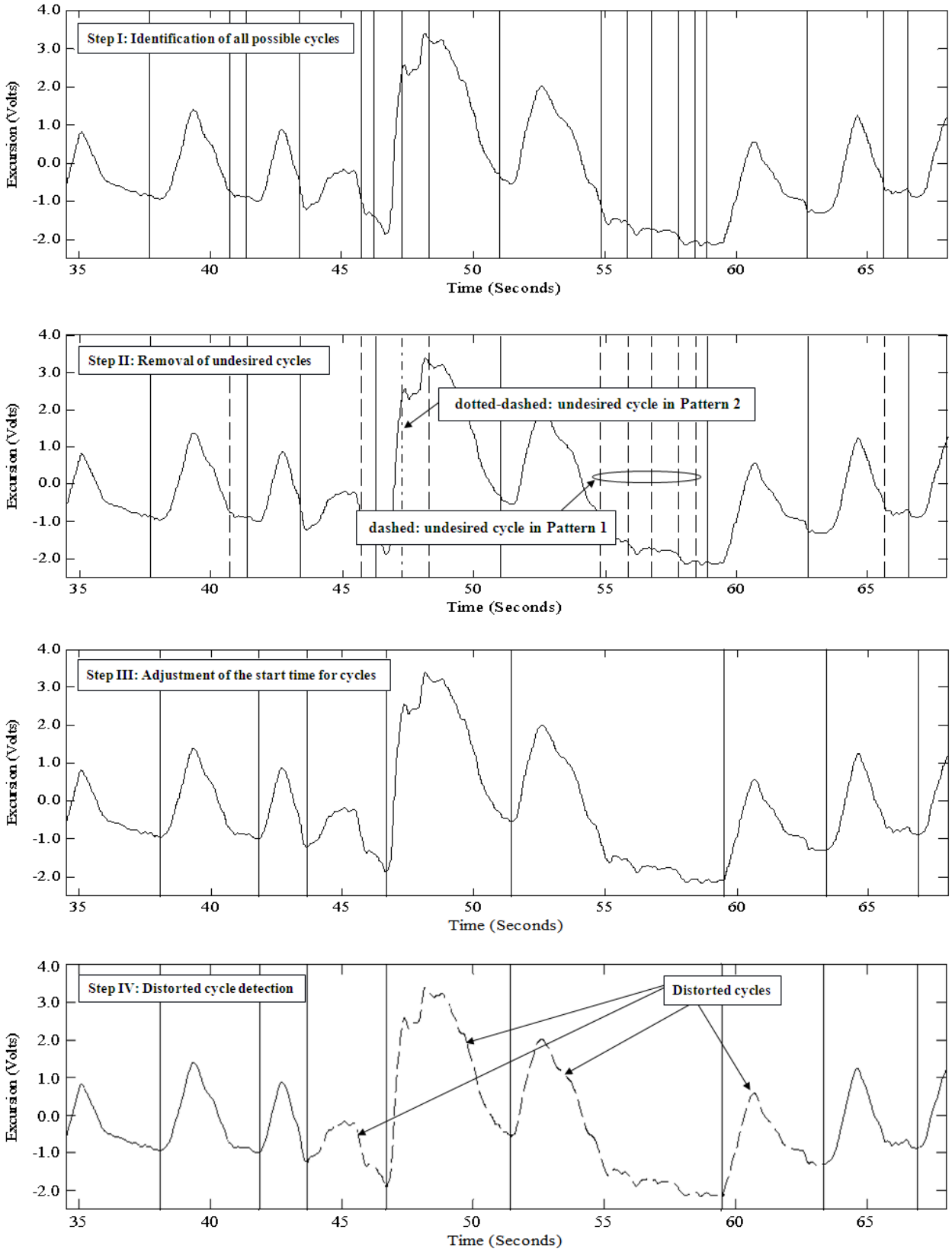

Figure 5. Corresponding cycle identification results of automatic cycle identification algorithm

3.2 Detailed Description of the Algorithm

3.2.1 Step I. Identification for All Possible Cycles

Although the respiratory signals can be considered as quasiperiodic with each cycle resembling a sinusoidal-squared waveform, the time duration for each cycle is not a fixed constant. Furthermore, the excursion voltage values at the end of expiratory phases often have small magnitudes yet fluctuate rapidly. This observation motivates us to use derivation as an initial means to identify the start time for the possible cycles. As demonstrated in Figure 6, the start time for the -th cycle is identified by a vertical line located at time , where subscript "I" denotes Step I. In the proposed algorithm, the signal was decimated by a factor of 30. Interpolation is performed on the decimated respiratory signal to recover the original time duration.

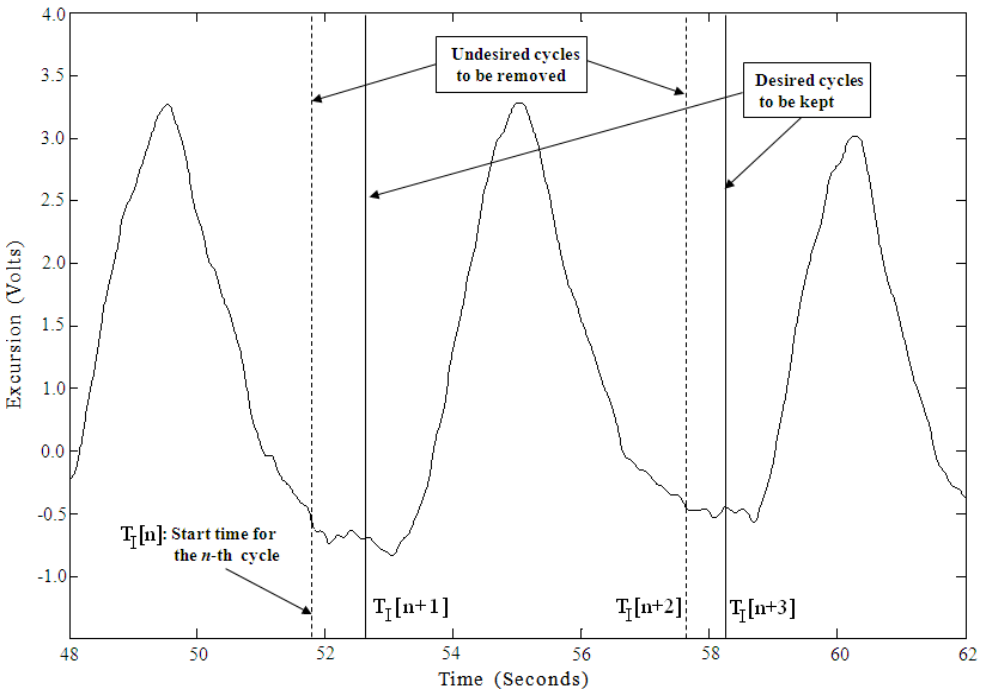

Figure 6. Step I of automatic cycle identification algorithm

As mentioned earlier, the signals in the trough between the expiratory phase and the following inspiratory phase usually do not possess any mathematically tractable waveforms.

Furthermore, the signals are bumpy if there is negligible motion artifact in the trough (see Figure 2). As a result, by taking the derivative of the respiratory signal, these small bumps are identified as cycles by Step I as shown by dashed lines in Figure 6. It is clear that these cycles do not represent the desired cycles and they are false or undesired cycles. Extra processing is needed to remove those undesired identification lines. This task is carried out in Step II.

To describe further steps, the following measurements are introduced associated with Step A. Figure 7 illustrates these measurements.

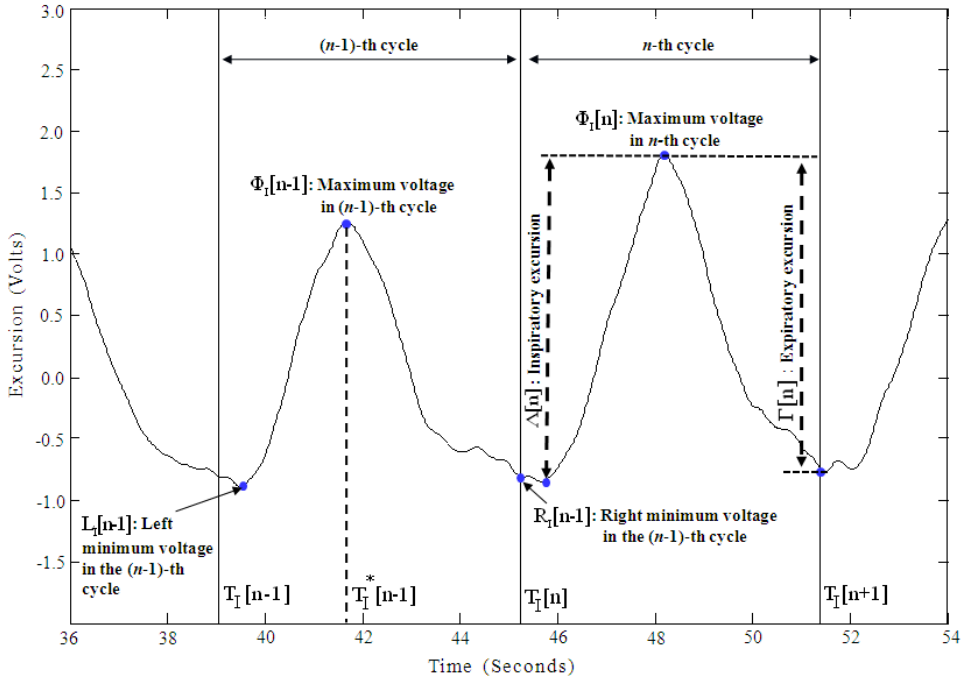

Figure 7. Example of cycle measurements

Maximum excursion voltage in the -th cycle:

, where and is, respectively, obtained in Step A. The time at which the maximum voltage occurs is denoted by , i.e., .

Minimum excursion voltage in the inspiratory phase in the -th cycle:

. As the inspiratory phase is in the left portion of a tidal cycle, it is referred to as the "left minimum".

Minimum excursion voltage in the expiratory phase in the -th cycle: . It is also referred to as the "right minimum".

Inspiratory excursion in the -th cycle: . It is calculated by the difference between maximum excursion voltage and left minimum voltage .

Expiratory excursion in the -th cycle: . It is calculated by the difference between maximum excursion voltage and right minimum voltage .

3.2.2 Step II. Removal of Undesired Cycles

The goal of this step is to remove the undesired cycles identified in Step I. It is observed that identification lines for these undesired cycles are typically drawn either at the trough between two desired adjacent cycles if there are bumps in the trough, or inside a cycle if there are small dips in the inspiratory or expiratory phases in a normal tidal breath cycle.

The undesired cycles can be classified into two patterns. Pattern 1, the undesired cycles that are located in the trough between two adjacent normal tidal breath cycles and the voltage difference between the maximum and minimum voltage in these undesired cycles is much smaller than those in desired tidal breath cycles. Figure 8 shows two undesired cycles (marked by dashed lines) in Pattern 1. This pattern occurs when participants have longer expiratory tail and the expiratory voltages fluctuate more rapidly with many small "bumps." As a result, more than one undesired cycles are often identified by Step I due to the multiple bumps. In the other pattern, the undesired cycles are typically located at the inspiratory phase of a distorted cycle which has severe artifacts. This pattern is referred to as Pattern 2. Figure 9 illustrates this pattern marked by a dashed line. To remove the undesired cycles in these two patterns, the following two criteria are implemented.

1) Criterion 1: One of the characteristics in the undesired cycles in Pattern 1, as shown in Figure 8, is that the voltage difference between the maximum and minimum voltage in the undesired cycles is very small compared with that in the desired cycles.

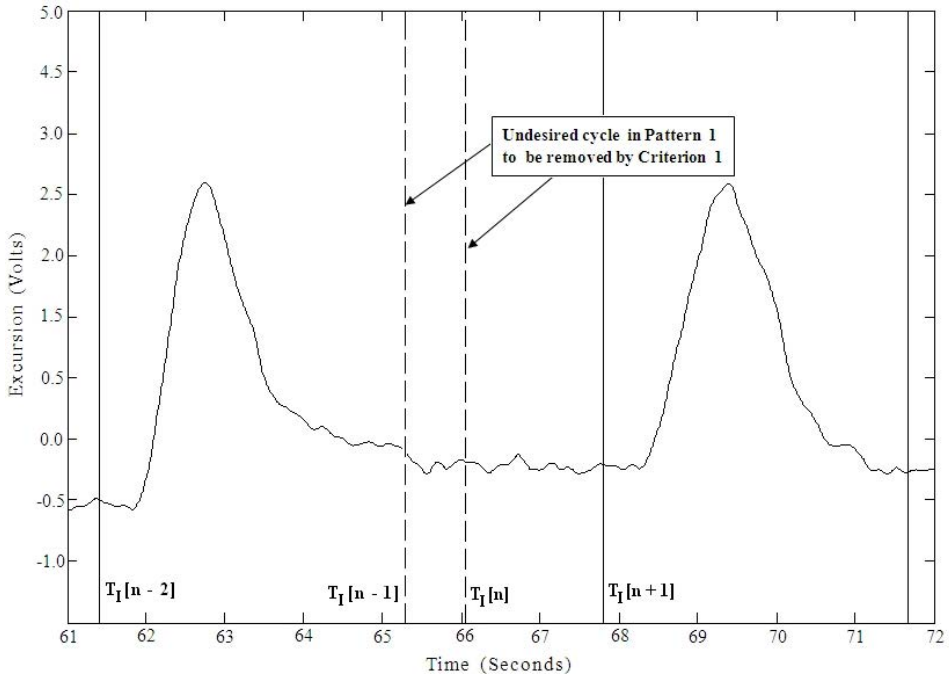

Figure 8. Criterion 1 for Pattern 1 in Step II of automatic cycle identification algorithm

Cycles in this pattern can be identified by examining the inspiratory excursion for each cycle and comparing it with the ensemble average. If the excursion for a cycle falls below a certain percentage of the average, the cycle is declared as undesired and its identification line is removed. After all the undesired cycles in this pattern are identified and removed, the cycle indexes are renumbered and the total number of cycles are . Criterion 1 is written as:

Where , and is the updated start time for the -th cycle in Step II Criterion 1, "null" represents the action that the identification line is removed,

— , is the ensemble average for the inspiratory excursion calculated over all cycles identified by Step I. The threshold is chosen as 37% in the algorithm.

2) Criterion 2: The undesired cycle in this pattern is located in the inspiratory phase, as illustrated in Figure 9, the -th cycle is undesired. The expiratory excursion (the difference between maximum and right minimum voltage) in the previous cycle, i.e., the -th cycle, must be much smaller compared to that in the -th cycle.

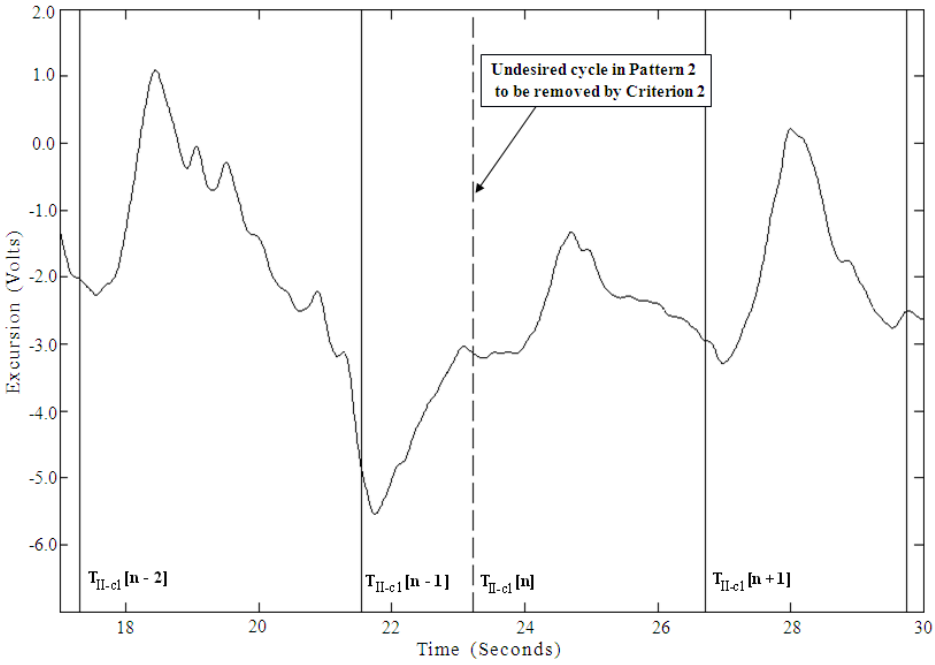

Figure 9. Criterion 2 for Pattern 2 in Step II of automatic cycle identification algorithm

Cycles in this pattern can be identified by comparing the ratio of expiratory excursions between the -th and -th cycles with the ensemble average value. If the ratio is larger than the ensemble average, then the -th cycle is identified as undesired and is removed. Similar to Criterion 1, after all the undesired cycles in this pattern are identified and removed, the cycles are renumbered according to the updated results. Criterion 2 is expressed as:

where , and ——— is the average for ratio of the expiratory excursions between a cycle and the previous one. The threshold is set as 8 in the algorithm. Here, we use , instead of to indicated the updated start time for the -th cycle, as there is no more criterions in Step II.

As a summary for Step II, after completing Criterion 1 and 2, all the undesired cycles have been removed and the total numbers of desired cycles and their identification lines have been identified. Each tidal breath cycle is marked by the time-instant at which the inspiratory phase begins. We use notation to represent the updated start time in the -th cycle. However, as observed in Figure 8 and Figure 9, the start times identified so far are still away from the exact start time of the cycles. The offsets usually represent very small amounts of time; we propose the following two-stage procedure in Step III to perform a final adjustment.

3.2.3 Step III. Adjustment on Start Time for the Cycles

The offsets in start time specified in Step II often occur in situations where there are many small dips or ripples in the ending segment of the expiratory phases. Consequently, the cycle identification lines are drawn between these dips, not at the exact start time of a cycle. Because of the variability in the ending segments of the expiratory phases, it is hard to specify the exact start times using a single criterion. However, the start times are observed to have one or more following features: (a) excursion voltage after the start time is consistently increasing, which is an indication of the next inspiratory phase, and (b) the excursion voltage at the start time has a locally mathematical minimum or near-mathematical minimum (near-mathematical minimum is referred as a value that is so close to the mathematical minimum that the difference cannot be detected visually). This motivates us to implement a two-stage procedure to perform a

final adjustment on the cycle identification lines such that the exact start time for each cycle can be successfully determined.

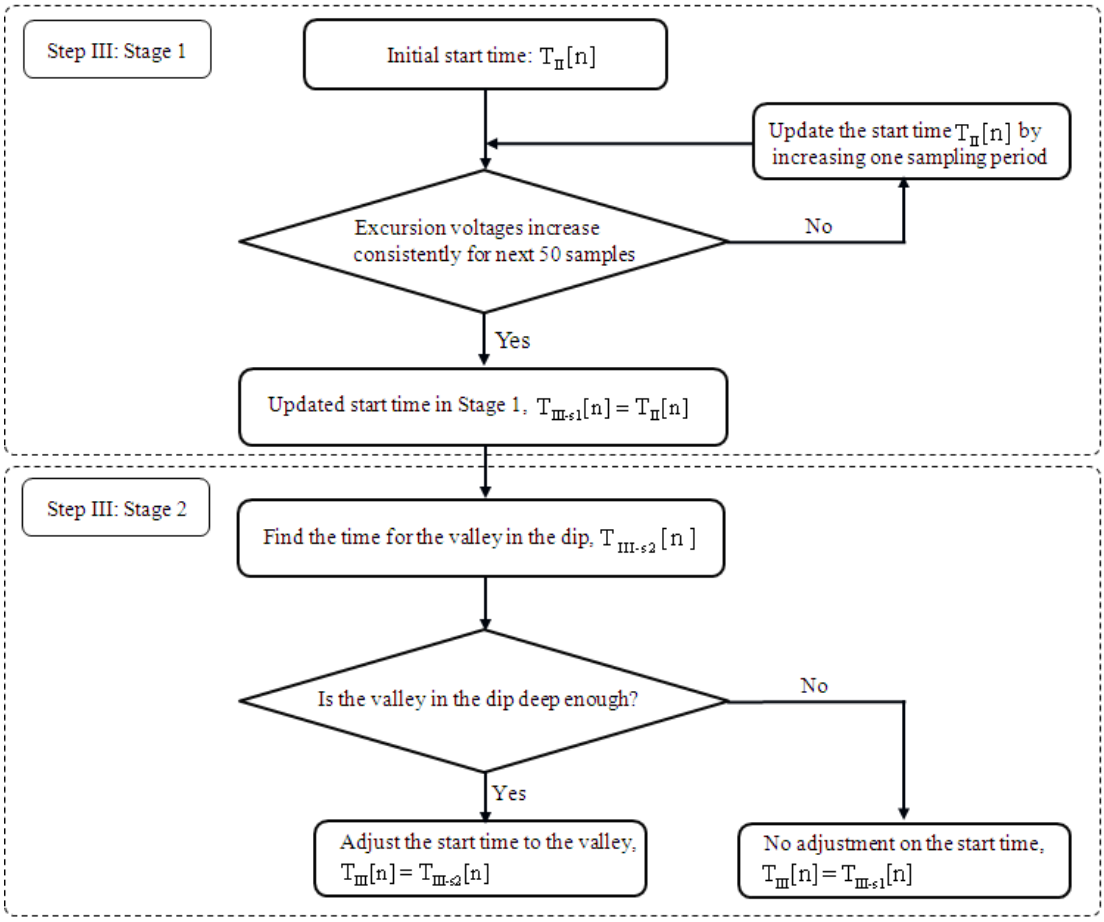

Figure 10. Diagram of Step III

In the first stage, the time after which the excursion voltage increases consistently is identified. Such time-instants happen to be the exact start times for most of the cycles, except for those in which the ending segment between previous expiratory phase and next inspiratory phase has a dip with an excursion small enough that can be treated as the start time of the cycles. In that case, the time-instants adjusted by the first stage are often over-adjusted. Stage 2 is introduced to undo the over-adjustment by identifying the dip with a larger drop in the excursion in the ending segment of the expiratory phase. The procedure of these two stages is illustrated in Figure 10. The details of these two stages are described as follows.

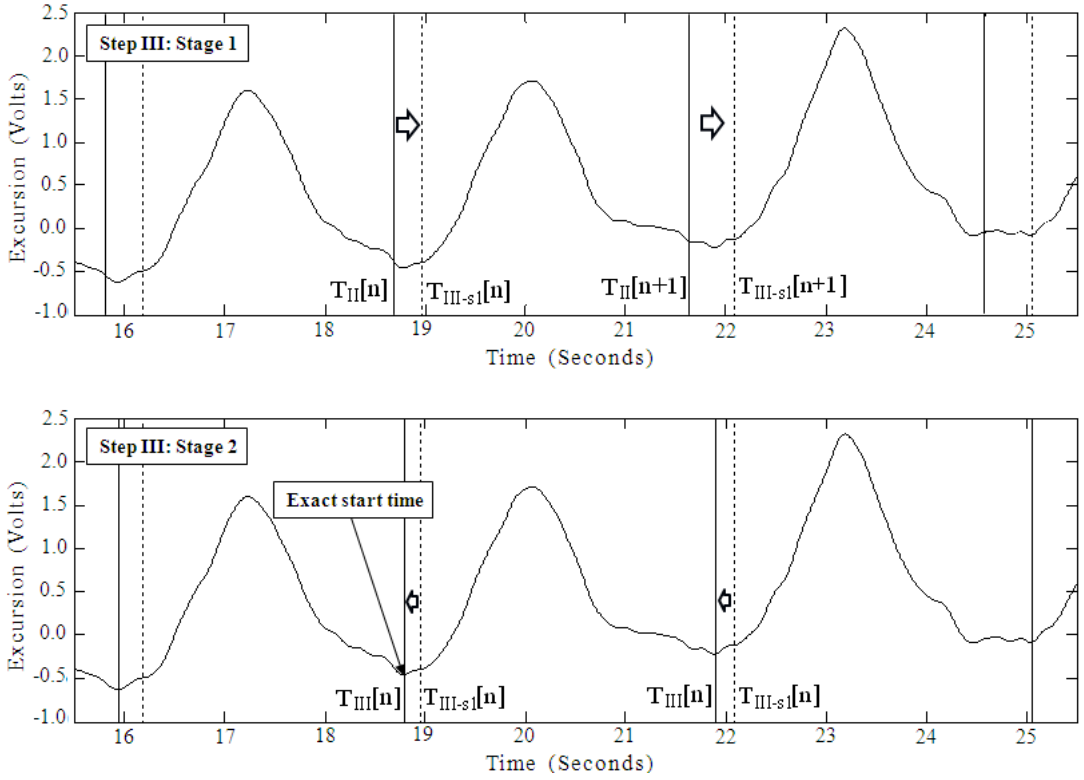

Figure 11. Stage 1 and Stage 2 of Step III of automatic cycle identification algorithm

1) Stage 1: In this stage, it needs to search for the time-instant at which the inspiratory phase starts and the excursion voltage increases consistently over a certain number of samples. Consistent 50 samples are chosen in the algorithm, which is half of a second (500 ms). The diagram for Stage 1 is shown in Figure 10. The search is performed for each cycle using the start time obtained in Step II to begin with. The next 50 samples of data are examined. Unless the voltages at those samples show a clear increasing trend consistently, there must be some dips in those samples. In this case, the cycle start time increased to one sample period and next 50 samples are examined from the updated start time. This procedure is repeated until a time-instant is found such that the voltages in the next 50 samples increase consistently.

The first plot in Figure 11 demonstrates the results from this stage. The start times for the -th and -th cycle are, respectively, updated by vertical dotted lines to the time-instants

and . It can be seen from the figure that start times for some cycles identified in Stage 1 are over-adjusted by a small time period from the correct desired start times. The reason is that there is often a dip in the trough with an excursion voltage lower compared with the excursion at the start time specified in Stage 1. Depending on how deep the dip is, it should be considered as part of the current cycle's inspiratory phase. Otherwise, it is considered part of the previous cycle's expiratory phase.

In Stage 1, a start time is identified as a point as which excursion voltages in the next 50 samples increase consistently. As a result, all ripples or bumps are excluded from the current cycle's inspiratory phase, and included in the previous cycle's expiratory phase. Consequently, the start time is over-adjusted. Further adjustments are performed in Stage 2.

2) Stage 2: In this stage, the over-adjusted start times for the cycles specified in Stage 1 are adjusted to the correct ones. As shown in the diagram of State 2 in figure 10, first the valley of the dip is located in the trough by finding the local minimum prior to the start time obtained in Stage 1. This is performed by a back-search for a decreasing trend in the excursion voltage until the time prior to which the voltage increases is found. Notation is used to represent the time at which the valley is located. Next, if the dip is deep enough, it is determined such that the cycle identification line should be moved to the valley in the dip. Use the local maximum voltage from the valley to the start time obtained in Stage 1 as a reference, it needs to check if the voltage difference between the local maximum and that in the valley is much bigger than the difference between the local maximum and the voltage at the start time obtained in Stage 1. In the algorithm, the ratio of the two voltage differences is used. If the ratio is bigger than a threshold , then the start time of the cycle is adjusted to the valley in the dip, otherwise, no adjustment.

Denote the local maximum is given by

. Stage 2 can be expressed by

where , and is the voltage difference between the local minimum and that in the valley, and is the difference between the local maximum and the voltage at the start time obtained in Stage 1.

The result from this stage is illustrated in the second plot in Figure 11. The final start times identified in Stage 2 in Step III are represented, respectively, by solid lines at and . For comparison, the results from Stage 1 are also plotted as dotted line and . It can be observed from the figure that the start times identified in Stage 2 indeed represent the correct desired time times.

3.2.4 Step IV. Distorted Cycle Detection

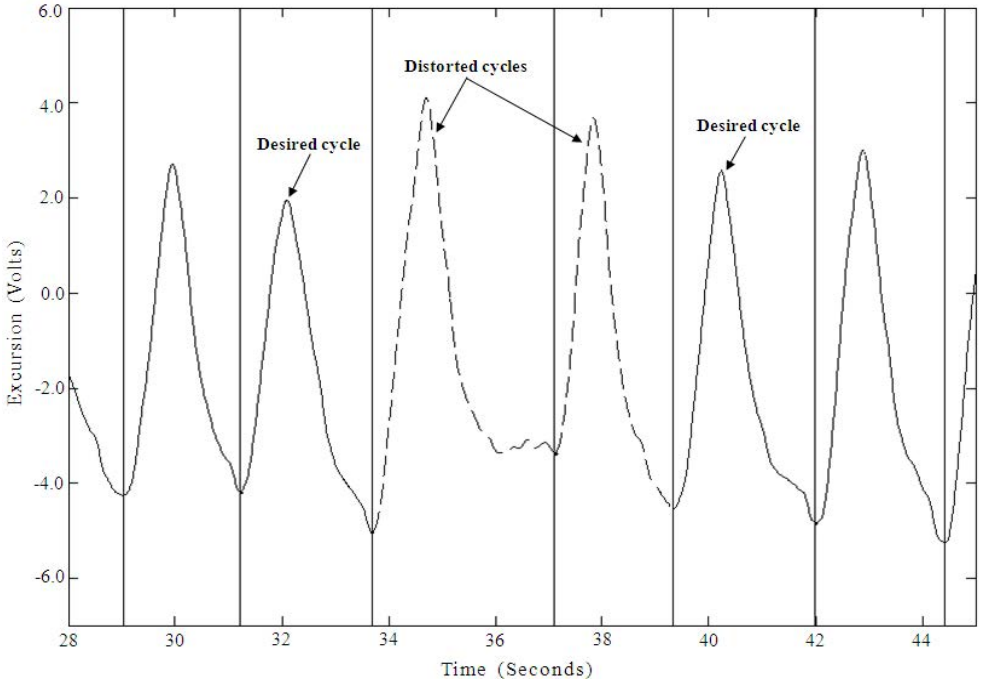

Figure 12. Example of distorted cycle detection

Even though the average shape of tidal breath cycles varies among and within participants, distorted cycles are characterized by one or more of the following when compared to typical tidal breath cycles: notably shorter durations, remarkably larger or smaller excursions, the presence of rapid signal deflections, and upward or downward trends within the signal that create a noticeable difference in the start and end voltages.

The distorted cycles can be detected by calculating the slope in each cycle, and the equation can be written as . If the absolute value of a cycle's slope is larger than a threshold , which is set to 0.19 in the algorithm, the cycle is declared distorted and is not used in further analysis. Figure 12 shows the results for the proposed scheme in distorted cycle detection. The distorted and non-distorted cycles are presented, respectively, by dashed and solid signal traces. The slope in the -th is larger than and that in the -th cycle is smaller than , they are thus determined as distorted cycles.

CHAPTER 4

SIMULATION

In this section, we compare the results of the automatic cycle identification algorithm with those of the hand-coded method. We provide simulation results using the proposed algorithm. The respiratory signals used for this comparison are described in Section II.

To identify tidal breath cycles using hand coding, an experienced coder viewed each respiratory signal as a time waveform within Time-Frequency Analysis for 32-bit Windows software [14]. Each cycle's initial and final points were identified using the waveform information. The software's label utility was used to mark the cycle's boundaries. The precision of the measurement was increased by zooming in on the cycle's initial and final points on separate passes and marking these points. The time required to code one signal by hand ranged approximately from 10 to 15 minutes, depending on the complexity of the signal.

The automatic cycle identification algorithm, described in Section III, was used to identify cycles in the same respiratory signals used for the hand-coded method. The threshold values and constants applied in the algorithm are listed in Table 1.

TABLE 1

CRITERIA PARAMETERS

Parameter	Meaning	Value
	Scalar of the subtraction between maximum and left minimum excursion voltage of the -th cycle.	0.37
	Scalar of the subtraction between maximum and right minimum excursion voltage of two adjacent cycles.	8
	Threshold for modification of cycle identification lines in stage 2, Step III.	10
	Threshold for distorted cycle detection.	0.19

The cycles identified by both ACIA (solid lines) and HCM (dashed lines) were plotted together on each respiratory signal (Figure 13). In some cases, both methods identified the same start time. In other cases, a zoomed-in review of the start times indicated that the ACIA more accurately identified the appropriate point than the HCM, due primarily to the resolution with which the algorithm could analyze the signal.

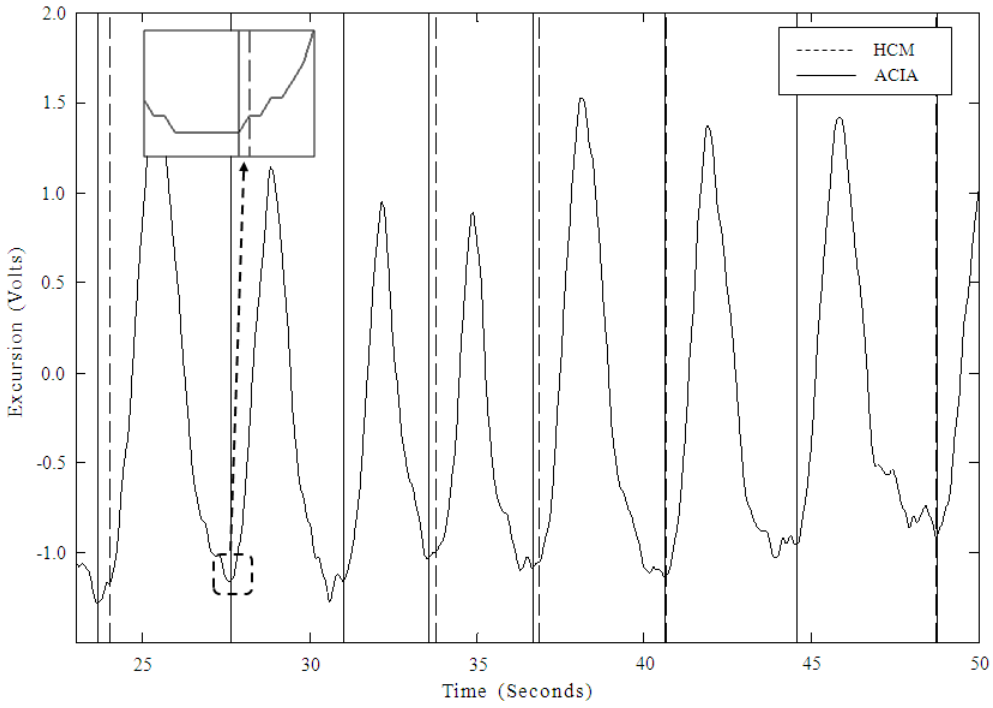

Figure 13. Example comparison of the automatic cycle identification algorithm and the hand-coded method on a filtered signal

In order to compare ACIA with HCM more exactly, we evaluate the duration of all cycles in the respiratory signals made by these two algorithms. A large-scale view of Figure 13 suggests three examples in which the two methods identified the same cycle start times. When the signal resolution is increased, as in the inset in the upper left-hand corner of the figure, a discrepancy between the methods becomes apparent.

The ACIA and HCM results were quantitatively compared using a sample of 211 tidal cycle start times. The ACIA results were identical to those of the HCM results 52 times (24.6%),

within 10 ms of the HCM results 125 times (59.2%), and within 40 ms of the HCM results 9 times (4.3%). In the remaining 25 cases (11.8%), the difference between the two methods ranged from 100 ms to 440 ms. These discrepancies were due to the fact that the ACIA was better able to resolve inspiratory start times than the hand coder. In 209 cases (99.1%), the AICA either replicated or more accurately identified the correct start time of the cycle than the HCM. Figure 14 illustrates the comparison result.

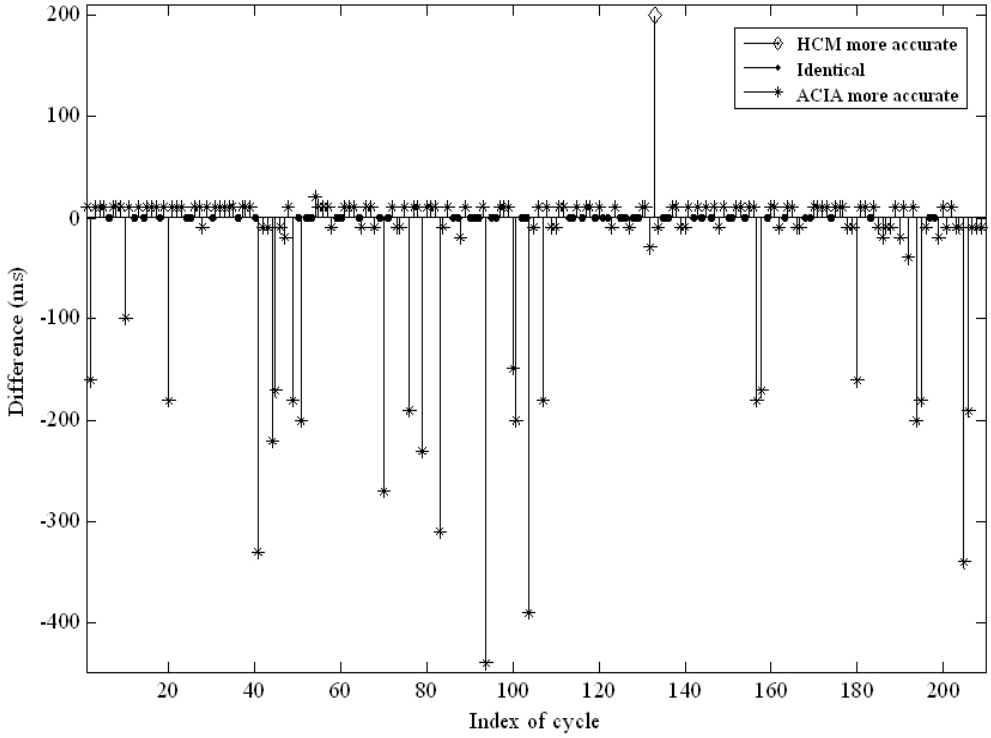

Figure 14. Difference between the automatic cycle identification algorithm and the hand-coded method

CHAPTER 5

CONCLUSION AND FUTURE WORK

We have developed a novel technique for automatically identifying respiratory cycles. Given the complexity of the respiratory signals, the results of the automatic cycle identification algorithm (ACIA) are promising. The algorithm surpassed the hand-coded method. It provides not only a time-saving method for coding respiratory signals, but also improves the accuracy with which the individual cycles are identified. In summary, compared to the results performed by an experienced hand-coder, the ACIA is able to more quickly select respiratory cycles, more accurately identify the start times of tidal breath cycles, and more efficiently code those start time cycles so that they can be used in subsequent analyses.

Future work will adapt the consider applying ACIA to different kinds of respiratory signals, such as those representing respiratory support for speech production. The respiratory signals for this type of breathing are distinctly different in shape, rate, and meaning than those for tidal breathing. As a result, the ACIA developed for tidal breath cycle identification may not be adequate for finding speech breathing cycles. Another area of analysis related directly to this current study is automatic cycle identification when signals are more negatively impacted by motion artifact than those of adult listeners, such as when measuring respiration during gross motor movement and respiration by adolescents and infants.

REFERENCES

REFERENCES

[1] P. de Chazal, C. Heneghan, E. Sheridan, R. Reilly, P. Nolan, and M. O'Malley, "Automated processing of the single-lead electrocardiogram for the detection of obstructive sleep apnoea", *IEEE Trans. Biomedical Engineering*, vol. 50, no. 6, pp. 686-696, Jun. 2003.

[2] P. de Chazal and R.B. Reilly, "Automatic classification of ECG beats using waveform shape and heart beat interval features", *IEEE Int. Confer. Acoustics, Speech, and Signal Processing*, vol. 2, pp. II - 269-72, Apr. 2003.

[3] A. L. Motto, H. L. Galiana, K. A. Brown, and R. E. Kearney, "Automated estimation of the phase between thoracic and abdominal movement signals", *IEEE Trans. Biomedical Engineering*, vol. 52, no. 4, pp. 614-621, Apr. 2005.

[4] T. Ning and J. D. Bronzino, "Automatic classification of respiratory signals", *IEEE Engineering Proc. Annu. Int. Conf.*, vol. 2, pp. 669-670, Nov. 1989.

[5] X. Wang, K. Brown, H. Galiana, and R. Kearney, "Identification of single-breaths and respiration patterns by ribcage and abdomen signals", *IEEE 29th Annu. Proc. Bioengineering Conf.*, pp. 128-129, Mar. 2003.

[6] R. Bailon, L. Sornmo, and P. Laguna, "A robust method for ECG-based estimation of the respiratory frequency during stress testing", *IEEE Trans. Biomedical Engineering*, vol. 53, no. 7, pp. 1273-1285, Jul. 2006.

[7] O. Meste, B. Khaddoumi, G. Blain, and S. Bermon, "Time-varying analysis methods and models for the respiratory and cardiac system coupling in graded exercise", *IEEE Trans. Biomedical Engineering*, vol. 52, no. 11, pp. 1921-1930, Nov. 2005.

[8] X. Zhu, W. Chen, T. Nemoto, Y. Kanemitsu, K. Kitamura, K. Yamakoshi, and D. Wei, "Real-time monitoring of respiration rhythm and pulse rate during sleep", *IEEE Trans. Biomedical Engineering*, vol. 53, no. 12, pp. 2553-2563, Dec. 2006.

[9] P. Hult, B. Wranne, and P. Ask, "A bioacoustic method for timing of the different phases of the breathing cycle and monitoring of breathing frequency" *Medical Eng. and Physics*, vol. 22, no. 6, pp. 425-433, Jul. 2000.

[10] T. Pham Dinh, H. Perrault, P. Calabrese, A. Eberhard, and G. Benchetrit, "New statistical method for detection and quantification of respiratory sinus arrhythmia" *IEEE Trans. Biomedical Engineering*, vol. 46, no. 9, pp. 1161-1165, Sept. 1999.

[11] J. W. Hamner and J. A. Taylor, "Automated quantification of sympathetic beat-by-beat activity, independent of signal quality", *J. Appl Physiol*, vol. 91, no. 3, pp. 1199-1206, Sept. 2001.

[12] S. M. Schulz, E. Ayala, B. Dahme, and T. Ritz, "A MATLAB toolbox for correcting within-individual effects of respiration rate and tidal volume on respiratory sinus arrhythmia during variable breathing", *Behavior Research Methods*, vol. 41, no. 4, pp. 1121-1126, Nov. 2009.

[13] P. Varady, T. Micsik, S. Benedek, and Z. Benyo, "A novel method for the detection of apnea and hypopnea events in respiration signals", *IEEE Trans. Biomedical Engineering*, vol. 49, no. 9, pp. 36-942, Sept. 2002.

[14] P. H. Milenkovic, "*Time-frequency analysis for 32-bit Windows (TF32)*"[online]. Available: http://userpages.chorus.net/cspeech/index.html.